

# Oxidative dehydrogenation of ethane and propane over vanadia and molybdena supported catalysts

Eleni Heracleous, Maria Machli, Angeliki A. Lemonidou\*, Iacovos A. Vasalos

Department of Chemical Engineering, Aristotle University of Thessaloniki and Chemical Process Engineering Research Institute (CERTH/CPERI), PO Box 1517, University Campus, GR-54006 Thessaloniki, Greece

Received 26 November 2004; received in revised form 3 January 2005; accepted 4 January 2005

## Abstract

The catalytic performance of vanadia and molybdena catalysts with monolayer coverage supported on alumina and titania in the oxidative dehydrogenation (ODH) of ethane and propane was investigated. The surface structure of the  $\text{MO}_x$  species ( $M = \text{Mo}, \text{V}$ ) was investigated with laser Raman spectroscopy, while the acidity and reducibility of the materials were probed by temperature programmed  $\text{NH}_3$  desorption and  $\text{H}_2$  reduction, respectively. Testing of the materials showed that in both ethane and propane oxidative dehydrogenation, vanadia catalysts were much more active than the molybdena ones, irrespective of the support used. Comparison of the catalysts based on the support used, showed that titania-supported catalysts exhibit superior activity but inferior selectivity than the corresponding alumina-supported ones. Taking into account that the oxygen involved in the  $M\text{--O}$ -support bonds is kinetically relevant, the behavior of each catalytic system can be explained based on the electronegativity of each cation involved in these bonds. The apparent activation energies for ethane and propane ODH, derived from kinetic measurements, follow the reactivity of the samples. Despite the higher reactivity of propane at same reaction conditions, similar values of activation energy were calculated. The pre-exponential factors could be responsible for the lower reaction rates in ethane ODH.

© 2005 Elsevier B.V. All rights reserved.

**Keywords:** Oxidative dehydrogenation; Ethane; Propane; Molybdena catalyst; Vanadia catalyst; Titania; Alumina

## 1. Introduction

Ethene and propene, the most important building blocks of the petrochemical industry, are currently produced by the energy intensive process of steam cracking. The development of more selective single processes starting from readily available lower alkanes conforms to the need for sustainable development. Oxidative dehydrogenation of light alkanes has been a research topic of consistent interest from mid-1980s. The presence of oxygen raises the thermodynamic restrictions of dehydrogenation and the exothermic character of the reaction renders it an energetically efficient process. The development of efficient heterogeneous catalysts for the gas-phase oxidative dehydrogenation of alkanes is of great importance because of the economic benefits of using light paraffins for

the production of important base chemicals. However, the yield of alkenes on most of the catalysts used is not satisfactory, due to the side reactions leading to the formation of  $\text{CO}_x$  [1].

Most of the catalysts investigated so far are based on reducible metals, mainly Mo and V [2–4]. The ODH reaction of  $\text{C}_2\text{--C}_4$  alkanes over supported transition metal oxides proceeds through a Mars and van Krevelen mechanism, which involves reduction of the catalyst by the alkane with participation of the lattice oxygen, followed by re-oxidation with oxygen. As is well known, the catalyst performance depends on a number of factors, such as the chemical nature of the active oxygen species, the redox properties and the acid–base character, which in turn depend on transition metal loading, dispersion and support effects [3–6].

The different overall activities of reducible supported catalysts are most probably related to the influence of the support than to the structure of the active species [7,8]. The re-

\* Corresponding author. Tel.: +30 2310 996273; fax: +30 2310 996184.  
E-mail address: [alemonidou@cheng.auth.gr](mailto:alemonidou@cheng.auth.gr) (A.A. Lemonidou).

activity of the active metal sites is governed by the bonds formed with the support (and the activity of oxygen species in these bonds) during the chemical interaction of the surface hydroxyl groups and precursor salts. This in turn highly depends on the acid–base properties of the supporting material. The investigation of the catalytic properties of vanadia supported catalysts in propane ODH showed that more selective catalysts were obtained on basic metal oxide supports [6,9]. The presence of basic sites enhances the fast desorption of the produced olefins from the catalytic surface, resulting in higher selectivities. Additionally, according to Kung [10], the selectivity for dehydrogenation versus formation of oxygen-containing products is strongly affected by the ability of the catalyst to form C–O bonds with the surface hydrocarbon, which depends on the reactivity of the oxygen species, and the number of reactive oxygen available at the reaction site. Reducibility has also been claimed to greatly affect the catalytic performance. Reports in literature have correlated variations in ODH activity with the ease of reducibility of the  $\text{MO}_x$  species on different supports [11], while other studies do not support such a trend [12].

The oxidative dehydrogenation reactions of various alkanes share many similar features. The first step in all alkane oxidation reactions seems to be common and involves the breaking of a C–H bond, which is considered the rate-limiting step. The ability of alkanes to be oxidized increases with the number of carbon atoms in the hydrocarbon following the order  $\text{C}_2 < \text{C}_3 < \text{C}_4 < \text{C}_5$ , which parallels the order in decreasing strength of the weakest C–H bond of the molecule and the number of such bonds in the alkane molecule, in the cases where this weakest bond strength is the same [4]. However, the product distribution is greatly affected by the nature of the alkane fed. For instance, doping vanadia catalysts with basic promoters has a beneficial effect in *n*-butane oxidative dehydrogenation by increasing the olefin selectivity, while the opposite effect is observed when ethane is used as feedstock [13]. This can be interpreted in terms of the different acid–base interaction between the catalyst and the alkane. The acid character of a hydrocarbon decreases as the number of carbon atoms and/or the degree of saturation decrease. Thus, less acidic alkenes (more basic) require stronger basic catalysts to limit the interaction of the alkene with the catalytic surface and preserve the olefin from further degradation. Furthermore, catalytic results for the oxydehydrogenation of propane and *n*-butane on V–Mg–O catalysts suggest that depending on the size of the reactant, the distance between the selective sites on the catalytic surface can influence the selectivity in the ODH reactions [14].

In this study, we report catalytic results obtained with Mo and V catalysts supported on  $\text{TiO}_2$  and  $\text{Al}_2\text{O}_3$  for the oxidative dehydrogenation of ethane and propane. Our goal was to examine the effect of active metal at loadings equivalent to monolayer coverage and effect of support on the catalytic performance in the ODH of  $\text{C}_2$ – $\text{C}_3$  alkanes. The effect of the nature of the alkane is also discussed.

## 2. Experimental

### 2.1. Catalyst preparation

The supports employed were  $\text{TiO}_2$  (Norton, SA = 50.8  $\text{m}^2/\text{g}$ ) and  $\gamma\text{-Al}_2\text{O}_3$  (Engelhard, SA = 183.9  $\text{m}^2/\text{g}$ ). Prior to impregnation, the supports were crushed and sieved to a particle size of 106–180  $\mu\text{m}$ . Molybdenum oxide catalysts supported on titania and alumina were prepared by wet impregnation of the corresponding supports with hot aqueous solutions of ammonium heptamolybdate,  $(\text{NH}_4)_6\text{Mo}_7\text{O}_{24}\cdot 4\text{H}_2\text{O}$  (Fisher), to ensure full dissolution of the precursor. The nominal weight loading of  $\text{MoO}_3$  was 5 wt.% for the sample supported on  $\text{TiO}_2$  and 15 wt.% for the one supported on  $\text{Al}_2\text{O}_3$ . After impregnation, the solvent was removed by evaporation under reduced pressure and the resulting solid was dried overnight at 120 °C. The titania-supported catalyst was calcined in synthetic air at 480 °C for 4 h, while the alumina one was calcined at 650 °C for 6 h.

Vanadium oxide was deposited on the two supports by wet impregnation using aqueous  $\text{NH}_4\text{VO}_3$  (Merck) solutions. Oxalic acid (Riedel-de Haen) was added to the solutions ( $\text{NH}_4\text{VO}_3/\text{oxalic acid} = 1/2$  molar) to ensure dissolution of ammonium metavanadate precursor. The nominal weight loading of  $\text{V}_2\text{O}_5$  was 5 wt.% for the sample supported on  $\text{TiO}_2$  and 14 wt.% for the one supported on  $\text{Al}_2\text{O}_3$ . After impregnation and solvent evaporation, the samples were dried overnight at 120 °C. Calcination was conducted in synthetic air at 480 °C for 4 h and at 650 °C for 6 h, for the titania- and alumina-supported samples, respectively.

The catalysts are referred to as “*x*MS”, where *x* represents the weight percent of the metal oxide, M the metal oxide used (Mo for  $\text{MoO}_3$  and V for  $\text{V}_2\text{O}_5$ ) and S the support used (Ti for  $\text{TiO}_2$  and Al for  $\text{Al}_2\text{O}_3$ ).

### 2.2. Catalyst characterization

The surface area of the samples was measured by  $\text{N}_2$  adsorption at 77 K, using the multipoint BET analysis method with an Autosorb-1 Quantachrome flow apparatus. The samples were dehydrated in vacuum at 250 °C overnight, before surface area measurements.

A Siemens D500 diffractometer, using Cu  $\text{K}\alpha$  radiation, was employed for obtaining the X-ray diffraction (XRD) patterns of the materials under study.

For the laser Raman spectroscopy measurements, each catalyst was pressed into a self-supporting wafer and placed in a sample holder consisting of a gold plate attached to a heating wire. The sample holder was mounted in the center of a Raman cell connected to a flow system. Prior to Raman spectra recording the samples were treated in helium flow at 120 °C for 1 h. Raman spectra were collected at 20 °C with a Renishaw Raman Spectrometer (Type 1000) equipped with a CCD-detector using a 785 nm diode laser excitation. The power level of the laser was 200 mW. The wave number accuracy was within 1  $\text{cm}^{-1}$ .

Temperature programmed reduction (TPR) experiments with  $H_2$  were carried out in a gas flow system equipped with a quadrupole mass analyzer (Omnistar, Balzers). Catalyst sample (0.2 g) was placed in a U-shape reactor and pretreated in flowing He for 0.5 h at 500 °C, followed by cooling at room temperature. The inlet total flow (5%  $H_2$  in He) was 50 cm<sup>3</sup>/min and the temperature was increased linearly at a rate of 15 K/min from 30 to 700 °C. The main ( $m/z$ ) fragments registered were:  $H_2 = 2$ ,  $H_2O = 18$  and  $He = 4$ .

$NH_3$ -temperature programmed desorption (TPD) was used to determine the acid properties. In a typical experiment, 0.1 g of the sample were loaded in a U-shape quartz reactor, pretreated at 500 °C for 0.5 h and then cooled to 100 °C under He flow. The pretreated samples were saturated with 5%  $NH_3$ /He for 1 h at 100 °C, with subsequent flushing at 100 °C for 1 h to remove the physisorbed ammonia. TPD analysis was carried out from 100 to 700 °C, at a heating rate of 10 K/min. The composition of the exit gas was monitored on-line by a quadrupole mass analyzer (Omnistar, Balzers). The  $m/z$  fragments registered were as follows:  $NH_3 = 15$ ;  $H_2O = 18$ ;  $N_2 = 28$ ;  $NO = 30$ ;  $N_2O = 44$  and  $NO_2 = 46$ . Quantitative analysis of the desorbed ammonia was based on  $m/z$  15.

### 2.3. Measurements of catalytic performance

The catalytic performance of the samples was measured in a fixed-bed quartz reactor. The catalyst particles were diluted with equal amounts of quartz particles of the same size to achieve isothermal operation. The temperature in the middle of the catalytic bed was measured with a coaxial thermocouple. The samples were activated in oxygen flow at 500 °C for 30 min. The composition of the reaction mixture used for experiments with ethane as feedstock was  $C_2H_6/O_2/He = 9/9/82$ , while for experiments with propane  $C_3H_8/O_2/He = 4.7/4.7/90.6$ .

The oxidative dehydrogenation was investigated in the temperature range from 250 to 600 °C. In order to obtain different alkane conversion levels at constant reaction temperature, the  $W/F$  ratio was varied from 0.002 to 0.36 g s cm<sup>-3</sup>. The reaction products were analyzed on-line by a Varian 3700 gas chromatograph equipped with a thermal conductivity detector (TCD). Two columns in a series-bypass configuration were used in the analysis: a Porapak Q and a MS 5A. Negligible amounts of oxygenates were observed at the reactor exit. The alkane conversion and the selectivity to the reaction products were calculated on a carbon basis.

The contribution of gas-phase reactions was tested by conducting experiments using an empty-volume reactor. The conversion of ethane and propane at these experiments was lower than 2% at 600 °C for ethane and 550 °C for propane, confirming that gas-phase reactions are negligible at the experimental conditions used for the activity tests.

Table 1  
Physicochemical characteristics of the catalytic samples

Catalyst	Metal oxide loading (wt.%)	BET surface area (m <sup>2</sup> /g)	Theoretical surface coverage, $\theta$
5MoTi	5	45.9	1.05
15MoAl	15	160.8	0.88
5VTi	5	43.0	0.97
14VAl	14	126.2	1.01

## 3. Results

### 3.1. Catalyst characterization

The characteristic properties of the catalytic materials prepared are shown in Table 1. The surface area of the samples varies from 43 to 160.8 m<sup>2</sup>/g. This large variation is mainly due to the initial difference in the surface area of the supports used (50.8 m<sup>2</sup>/g for TiO<sub>2</sub> and 183.9 m<sup>2</sup>/g for Al<sub>2</sub>O<sub>3</sub>). The MoO<sub>x</sub> theoretical surface coverage of the molybdenum-containing samples was calculated on catalyst surface area, using 22 Å<sup>2</sup> as the mean surface area occupied by one Mo<sup>6+</sup> oxide unit [15]. The VO<sub>x</sub> surface coverage was also calculated on catalyst surface area, on the basis that complete coverage of support surface with vanadium oxide needs 7.9 and 7.3V atoms/nm<sup>2</sup> for titania and alumina, respectively [7]. Theoretical surface coverage values around monolayer were obtained for both the titania and alumina samples.

Crystalline phases in the catalysts were characterized by X-ray diffraction. The diffractograms obtained are presented in Fig. 1. All samples exhibited diffraction lines characteristic of the supports used. No diffraction lines corresponding to Mo-containing compounds were detected in the molybdenum samples, indicating that the molybdena species are amorphous in nature and highly dispersed on the support surface. The same was observed with the vanadia on titania catalyst. However, with the alumina-supported V catalyst, it

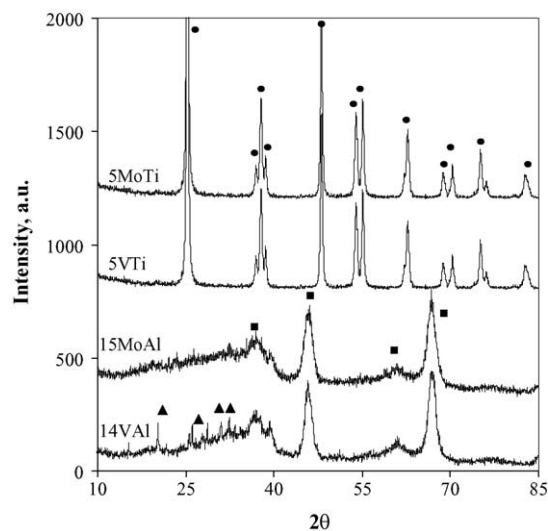


Fig. 1. X-ray diffraction patterns of the catalytic samples. The peaks are marked as: (●) TiO<sub>2</sub>, (■) Al<sub>2</sub>O<sub>3</sub> and (▲) V<sub>2</sub>O<sub>5</sub>.

is clear that even though the theoretical coverage is equal to monolayer,  $V_2O_5$  crystallites were formed and detected in the X-ray diffraction pattern of the sample.

Based on literature, three concepts of the term “monolayer” can be distinguished: (i) theoretical geometry monolayer, (ii) saturated adsorption monolayer and (iii) uppermost dispersion capacity monolayer [16]. The monolayer surface coverage is commonly defined as the maximum amount of amorphous or two-dimensional metal oxide in contact with the oxide support. From the V–O and Mo–O bond lengths of the crystalline  $V_2O_5$  and  $MoO_3$ , monolayer surface coverage is estimated to be 7–8V atoms/nm<sup>2</sup> [7] and 5Mo atoms/nm<sup>2</sup>, respectively [15,17]. In our case, for example, the  $VO_x$  density of 14VAI is 7.35V atoms/nm<sup>2</sup>, almost equal to the amount necessary for monolayer coverage. However, formation of crystalline  $V_2O_5$  was observed. The imperfect dispersion of vanadia on alumina can be attributed to the preparation conditions (preparation method, calcination temperature) and to the nature of the support. The presence of crystalline vanadia on alumina for similar vanadia loading was also reported by Khodakov et al. [18].

Raman spectra of the samples are shown in Fig. 2. The 5MoTi sample exhibits a Raman band at 994 cm<sup>-1</sup> assigned to the stretching mode of the terminal Mo=O bond, arising from monomeric and/or polymeric surface molybdena species [19,20]. The broad band from 900 to 800 cm<sup>-1</sup> centered at 850 cm<sup>-1</sup> is attributed to the stretching mode of Mo–O–Mo bonds of polymerized surface molybdenum oxide species in different configurations (dimers, oligomers, longer polymeric chains) [12,17,20]. The spectrum of 15MoAl is similar to that of 5MoTi with a band arising from Mo=O vibrations shifted to 1003 cm<sup>-1</sup> and a broad band at lower wavenumbers, arising from the bridging Mo–O–Mo mode. The absence of crystalline molybdena

(820 and 990 cm<sup>-1</sup>) or/and aluminum molybdate distinct bands confirms the high dispersion of molybdena species on both alumina and titania support.

The spectrum of 5VTi catalyst consists of a weak band at 1027 cm<sup>-1</sup> characteristic of the terminal V=O bond of both monomeric and polymeric vanadyl groups [18,19]. The broad band centered at 920 cm<sup>-1</sup> is due to V–O–V functionalities of polymeric species. The Raman spectrum of 14VAI possesses a blue shifted band at 1032 cm<sup>-1</sup> assigned to the V=O mode and an asymmetric broad band in the 920–850 cm<sup>-1</sup> range with a maximum intensity at 940 cm<sup>-1</sup>, which can be ascribed to both V–O–V polymeric functionalities and  $AlVO_4$  microcrystallites [21]. The formation of  $AlVO_4$  on high loading V/ $Al_2O_3$  catalysts calcined at temperature higher than 600 °C has been reported in literature [22]. The absence of diffractions characteristic of this mixed phase in the XRD pattern of the 14VAI catalyst is possibly due to the low concentration and/or size of the  $AlVO_4$  microcrystallites. The appearance of this phase in the Raman spectrum is due to the much higher sensitivity of Raman spectroscopy to crystallized materials. In addition to the aluminum vanadate phase, the strong characteristic bands at 994 and 700 cm<sup>-1</sup> indicate also the presence of crystalline  $V_2O_5$  [18,23]. The formation of crystalline phases on 14VAI indicates poor dispersion of vanadia species on the surface of alumina compared to titania.

The acidic properties of Mo- and V-containing catalysts investigated by  $NH_3$  TPD are compiled in Fig. 3. The intensity of the  $NH_3$  signal was normalized per surface area to account for the large variation in the surface areas of the catalytic materials studied. The main desorption product was in all cases  $NH_3$ , while traces of  $N_2$ , NO and  $N_2O$  were also detected. All samples are characterized by desorption profiles in the range 100–450 °C, with maximum temperature of

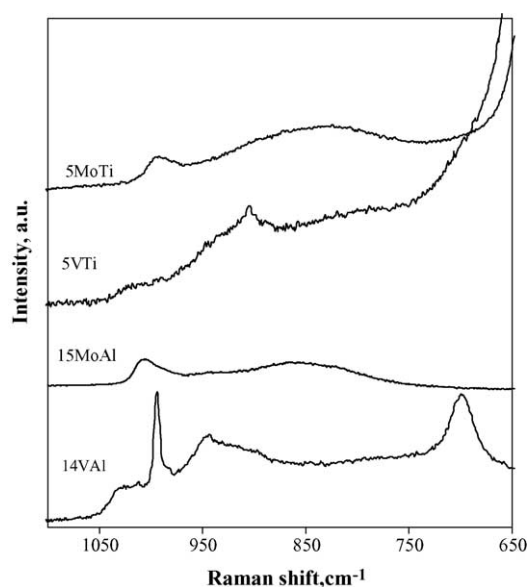


Fig. 2. Raman spectra of vanadia and molybdena catalysts supported on titania and alumina.

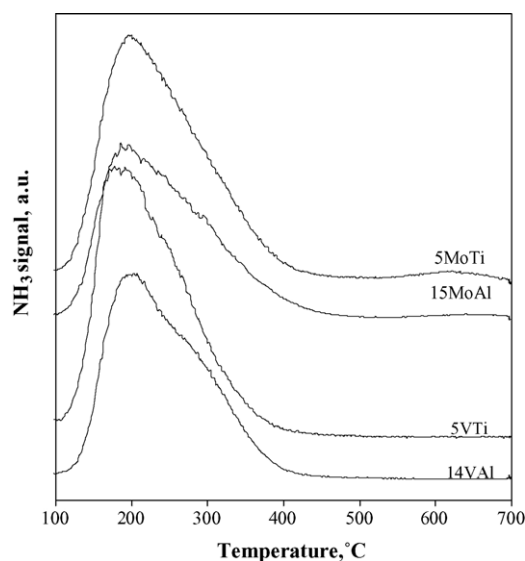


Fig. 3.  $NH_3$ -temperature programmed desorption profiles of the catalytic samples.

Table 2  
Acidity, reducibility and activation energy for ethane and propane ODH

Catalyst	Acidity ( $\mu\text{mol NH}_3/\text{m}^2$ )	$T$ reduction ( $^\circ\text{C}$ )	$E_a$ (ethane) (kJ/mol)	$E_a$ (propane) (kJ/mol)
5MoTi	8.73	491	104	97
15MoAl	6.64	488	91	87
5VTi	9.39	490	67	70
14VAI	7.13	524 and 630	85	80

ammonia desorption at  $\sim 200^\circ\text{C}$ . The  $\text{NH}_3$  desorption patterns suggest that acid sites of weak and moderate strength are present on the catalysts. The  $\text{TiO}_2$ -supported catalysts exhibit a more symmetric desorption peak, while a shoulder at  $\sim 280^\circ\text{C}$  is noticeable in the  $\text{NH}_3$  desorption curves of 15MoAl and 14VAI. This could indicate a higher fraction of acid sites of medium strength on the  $\text{Al}_2\text{O}_3$  supported catalysts. A small peak at high temperature ( $>600^\circ\text{C}$ ) observed for the 5MoTi sample can be ascribed to strong acid sites of small uncovered patches of the support.  $\text{MO}_x$  ( $M = \text{Mo}, \text{V}$ ) species supported on  $\text{TiO}_2$  exhibit in general higher acidity than the corresponding  $\text{Al}_2\text{O}_3$  supported ones (Table 2). The difference is due to the higher acidity ( $\mu\text{mol NH}_3/\text{m}^2$ ) of titania compared to that of alumina. On the same support, V catalysts are slightly more acidic than the corresponding Mo ones.

Temperature programmed reduction (TPR) with  $\text{H}_2$  is a useful technique to probe the reducibility of catalytic materials. The two supports used were also examined by TPR. A limited reduction at high temperature ( $>620^\circ\text{C}$ ) was observed for the titania support, while a flat  $\text{H}_2$  profile was obtained with alumina. The reduction profiles of the catalytic samples are presented in Fig. 4. Catalyst 5VTi shows a temperature of maximum hydrogen reduction at  $490^\circ\text{C}$ , whereas 14VAI exhibited two nearly distinct peaks at higher temper-

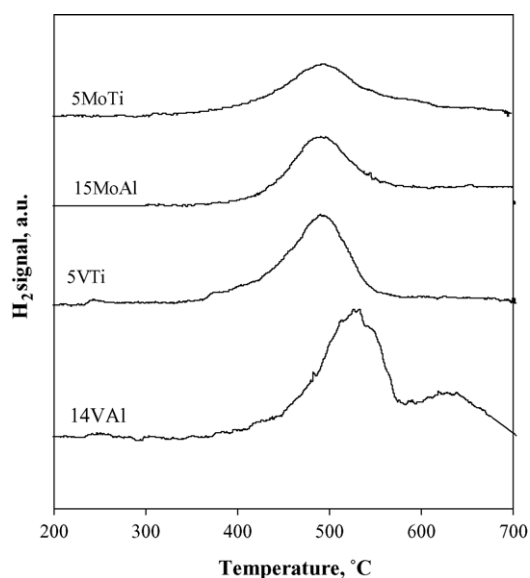


Fig. 4.  $\text{H}_2$ -temperature programmed reduction profiles of the catalytic samples.

ature than 5VTi ( $524, 630^\circ\text{C}$ ). Higher reduction temperature of vanadia–alumina than vanadia–titania catalytic system is also reported in literature [5,24]. The two peaks of 14VAI indicate the presence of at least two different forms of vanadia species on the alumina surface. At lower temperature, it is likely that amorphous, two-dimensional V species are reduced, whereas the peak at higher temperature is attributed to the reduction of crystalline  $\text{AlVO}_4$  and  $\text{V}_2\text{O}_5$ . Molybdena catalysts, 5MoTi and 15MoAl, exhibit almost the same temperature of maximum  $\text{H}_2$  consumption, indicating similar structural arrangements of molybdena species on both supports. According to the literature, molybdena on alumina catalysts exhibits two broad peaks, the low temperature peak corresponding to the reduction of  $\text{Mo}^{6+}$  to  $\text{Mo}^{4+}$  and the high temperature peak to the reduction of  $\text{Mo}^{4+}$  to  $\text{Mo}^0$  [11,25]. However, the reduction patterns derived from TPR experiments are very sensitive to the experimental conditions (flow rate,  $\text{H}_2$  concentration, heating rate, maximum heating temperature, etc.) and thus, the absence of the high temperature peak in our TPR profile could be due to the experimental conditions used ( $T_{\text{max}} = 700^\circ\text{C}$ ).

## 3.2. Catalytic results

### 3.2.1. Oxidative dehydrogenation of ethane

Two series of experiments were conducted in order to assess the performance of the titania- and alumina-supported Mo and V catalysts in the oxidative dehydrogenation of ethane. In the first series, the activity of the catalysts was measured as a function of reaction temperature. The experiments were run at a temperature range of  $250\text{--}600^\circ\text{C}$ , with constant gas flow ( $55\text{ cm}^3/\text{min}$ ), weight of catalyst ( $0.3\text{ g}$ ) and ethane/oxygen ratio (1/1). Activity is expressed as specific surface activity (SSAc) to account for the different surface areas of the supports used. The SSAc, expressed as  $\mu\text{mol C}_2\text{H}_6\text{ m}^{-2}\text{ s}^{-1}$ , is plotted in Fig. 5 as a function of reaction temperature. The activity per surface area decreases in the following order:  $5\text{VTi} \gg 14\text{VAI} > 5\text{MoTi} > 15\text{MoAl}$ .

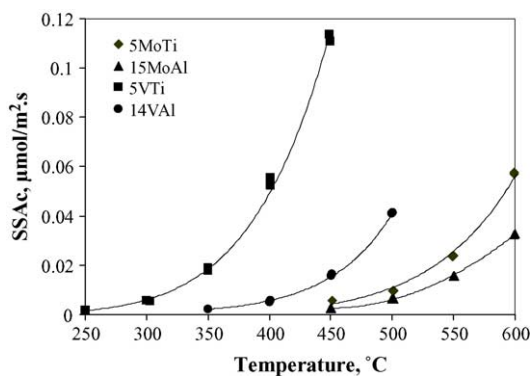


Fig. 5. Specific surface area activity (SSAc) as a function of temperature in ethane oxidative dehydrogenation (reaction conditions:  $W/F = 0.33\text{ g cm}^{-3}$ ,  $\text{C}_2\text{H}_6/\text{O}_2 = 1/1$ ).

Given that the catalysts have almost the same  $\text{MO}_x$  density, the intrinsic activities per V or Mo atom (TOF values) follow the same trend.

The results clearly indicate that V-containing catalysts are far more active than the corresponding Mo ones, irrespective of the supporting metal oxide. A comparison between the catalysts on the basis of the support used demonstrates the superior activity of the  $\text{TiO}_2$ -supported samples. The support effect is much more pronounced in the case of the V samples, where 5VTi exhibits almost 10 times higher reactivity than 14VAI in all temperatures studied. In the Mo catalysts, 5MoTi is approximately 2 times more active than 15MoAl. Burcham et al. also observed that the support effect in V catalysts led to turnover frequency (TOF, activity per vanadium site) differences spanning three orders of magnitude in the methanol oxidation reaction, while one order of magnitude difference in the TOF values was reported for Mo-containing catalysts in the same reaction [26].

The main problem associated with ODH catalysts is the decrease in olefin selectivity with increasing alkane conversion, consistent with a parallel–consecutive reaction network. Alkenes are highly reactive molecules, in most cases more active than the corresponding alkanes, and thus are easily activated by the catalytic surface and undergo secondary oxidation reactions to  $\text{CO}_x$ . In order to study the selectivity–conversion relation, we conducted a second series of experiments at constant temperature ( $550^\circ\text{C}$ ), constant ethane/oxygen ratio (1/1) and varying  $W/F$  from 0.01 to  $0.36\text{ g s cm}^{-3}$  in order to attain different conversion levels. The ethene selectivity versus ethane conversion is illustrated in Fig. 6. The results clearly demonstrate the inverse relation between selectivity and conversion, typical of the oxidative dehydrogenation reactions. Significant differences in ethene selectivity between the catalysts are observed. Selectivity to ethene decreases in the following order: 15MoAl > 5MoTi > 14VAI > 5VTi. It is clear that in the case of ethane ODH, the presence of  $\text{MoO}_x$  entities enhances the selective conversion of ethane to ethene, since Mo catalysts demonstrate significantly superior selectivity. The support nature also seems to affect selectivity to the de-

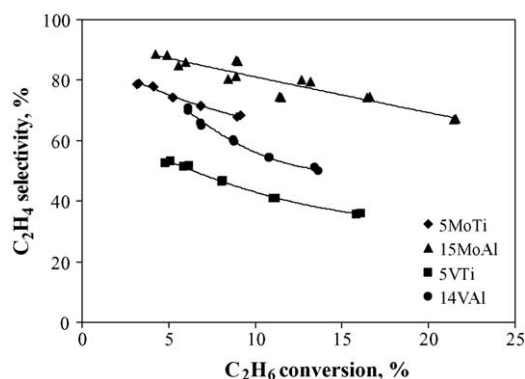


Fig. 6. Ethene selectivity as a function of ethane conversion (reaction conditions:  $T = 550^\circ\text{C}$ ,  $\text{C}_2\text{H}_6/\text{O}_2 = 1/1$ ).

sired olefin. Both Mo and V catalysts supported on alumina demonstrate an increase of at least 20% in ethene selectivity compared to the corresponding titania catalysts. A possible relationship between acidity and selectivity could exist. The surface concentration of acid sites on  $\text{MoO}_3/\text{TiO}_2$  is higher than on the  $\text{MoO}_3/\text{Al}_2\text{O}_3$  catalyst, as indicated by the  $\text{NH}_3$ -TPD results. A parallel trend is observed for the V-supported samples. The stronger interaction of ethane with more acidic  $\text{TiO}_2$  catalysts may well result in direct combustion of a higher fraction of ethane to oxidation products.

The decrease in ethene production with increasing ethane conversion follows an almost parallel trend for all catalysts, except for the 14VAI that exhibits a sharper drop in selectivity with conversion. The different behavior of the 14VAI catalyst can be attributed to the formation of  $\text{V}_2\text{O}_5$  crystallites, detected in the diffractogram of this sample. The parallel trends in activity and selectivity–activity relationship on the samples suggest that the oxidative dehydrogenation reaction follows the same mechanism over reducible  $\text{MoO}_x$  and  $\text{VO}_x$  supported catalysts.

### 3.2.2. Oxidative dehydrogenation of propane

The activity of the catalysts in propane ODH was measured in a temperature range from  $300$  to  $550^\circ\text{C}$ . In Fig. 7, the specific surface activity (SSAc), expressed as  $\mu\text{mol C}_3\text{H}_8\text{ m}^{-2}\text{ s}^{-1}$ , is plotted versus reaction temperature. It is clear that both the nature of metal oxide and the support used affect the activity which follows the series:  $5\text{VTi} \gg 14\text{VAI} > 5\text{MoTi} > 15\text{MoAl}$ .

As with ethane ODH, vanadia catalysts are significantly more active than molybdena ones. Similar results have also been reported for the oxidative dehydrogenation of propane by Grabowski et al. [27]. Vanadia on titania (5VTi) is a very active catalyst, far more active than vanadia on alumina (14VAI). Literature reports have correlated the high activity of vanadia–titania catalysts with the good dispersion capacity of the  $\text{TiO}_2$  support [28–31]. The presence of vanadia crystals on alumina even at loadings equivalent to monolayer coverage reduces the number of active sites available on the

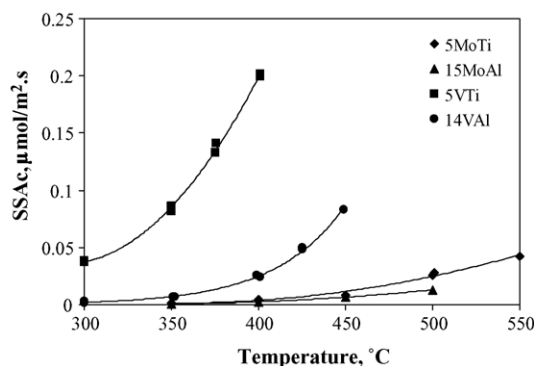


Fig. 7. Specific surface area activity (SSAc) as a function of temperature in propane oxidative dehydrogenation (reaction conditions:  $W/F = 0.06\text{ g s cm}^{-3}$ ,  $\text{C}_3\text{H}_8/\text{O}_2 = 1/1$ ).

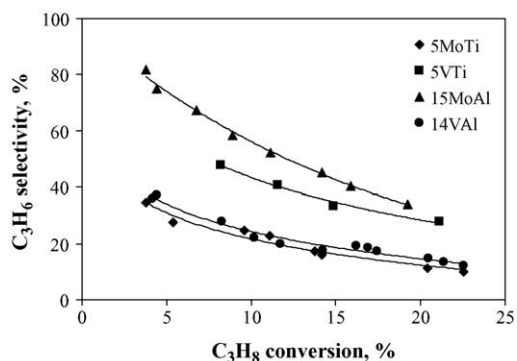


Fig. 8. Propene selectivity as a function of propane conversion (reaction conditions:  $T = 500^\circ\text{C}$ ,  $\text{C}_3\text{H}_8/\text{O}_2 = 1/1$ ).

catalytic surface, which is reflected in the lower activity of the 14VAI catalyst. In the case of Mo catalysts, the catalyst supported on titania (5MoTi) presents again better catalytic performance than the one supported on alumina (15MoAl), although the effect of support is not so pronounced as in vanadia catalysts.

In order to investigate the selectivity to propylene, experiments were conducted at  $500^\circ\text{C}$  using different  $W/F$  ratios. Selectivity to propylene as a function of propane conversion is depicted in Fig. 8 and the usual situation of propane ODH appears again, i.e., the selectivity to propylene drops as propane conversion increases. Propane and produced propylene undergo oxidation reactions, leading to the undesired formation of carbon oxides. The 15MoAl catalyst is the most selective one with initial propene selectivity over 80%. Noticeable decrease in propene selectivity is observed with the 5MoTi catalyst, especially at low conversion levels. Between vanadia catalysts, 5VTi exhibits higher selectivity than 14VAI. The low selectivity to propene of 14VAI can be attributed to the bulk  $\text{V}_2\text{O}_5$  present in the sample, which was found to be less selective in propane ODH [3].

### 3.2.3. Kinetic measurements

The reactivity of the catalysts is reflected in the activation energy, derived from kinetic measurements. The apparent activation energy for the materials under study was

calculated from Arrhenius plots (Fig. 9A and B) for ethane and propane consumption rates. Data were obtained from experiments performed at suitable conditions (temperature and  $W/F$  ratio) in order to obtain low conversion points ( $<10\%$ ). The values obtained in this work (Table 2) are comparable in magnitude as those reported in literature for similar catalysts [32].

In the oxidative dehydrogenation of ethane, the most active catalyst (5VTi) exhibits, as expected, the lowest energy required for the activation of ethane. The trend in activation energy parallels the ethane conversion (conversion attained at  $450^\circ\text{C}$  is given in brackets): 5VTi: 67 kJ/mol (37.9%) > 14VAI: 85 kJ/mol (17%) > 15MoAl: 91 kJ/mol (3.3%) > 5MoTi: 104 kJ/mol (2.2%).

The case is the same when propane is used as feedstock, with the calculated activation energies following the catalytic behavior during propane ODH. The lower the activation energy, the easier the C–H bond is activated and consequently the higher the catalytic activity in propane ODH. 5VTi catalyst exhibits the lowest activation energy and the highest catalytic activity.

Still, the noticeably different reactivity between the catalysts cannot be solely a result of the variation in the activation energy, which even though differs, spans in the same range ( $85 \pm 15$  kJ/mol) for all the catalysts. Since the activation energy of the samples is in the same order of magnitude, we could infer that the reaction rate is in a large part controlled by the pre-exponential factor. The pre-exponential factor depends on different parameters, such as the structure, the number of active sites and the activity per site. In view of the fact that the structure of the catalysts remains largely unaffected by the oxide support (see discussion below), the catalytic results indicate that differences in reactivity arise from the different number of active sites and/or the activity per site. We could say that in the case where the active metal is different (V or Mo), the activity per V site is higher than the corresponding per Mo site, thus resulting in the higher reactivity of the V-containing catalysts. In the case where the support is different, it could be possible that the number and/or the activity of the catalytic sites on titania is higher than on alumina.

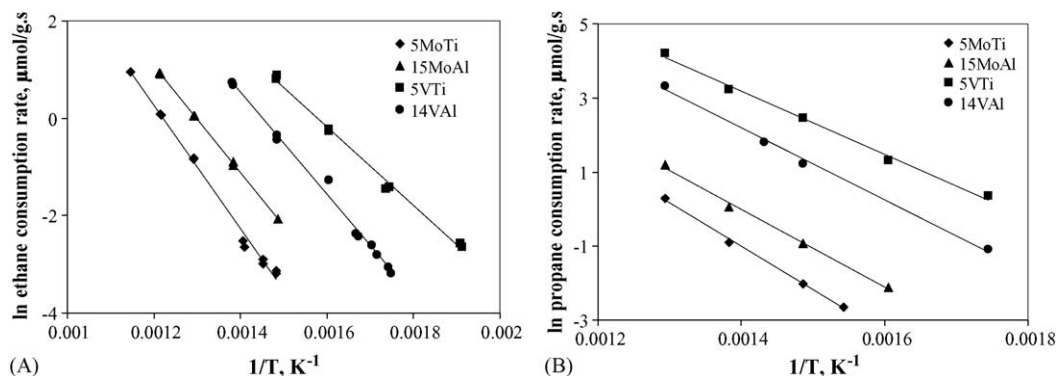


Fig. 9. Arrhenius plots for: (a) ethane ODH and (b) propane ODH.

## 4. Discussion

### 4.1. Effect of active metal oxide

The oxidative dehydrogenation reaction is suggested to proceed via a redox (Mars and van Krevelen) type mechanism in two steps, i.e., reduction of the catalyst by the alkane with extraction of the lattice oxygen, followed by re-oxidation of the reduced catalyst with molecular dioxygen. The significantly higher ODH rates (Figs. 5 and 7) measured over vanadia catalysts for both alkanes (ethane and propane) suggest that redox cycles occur more rapidly on  $\text{VO}_x$  than on  $\text{MoO}_x$  species [33]. The increased activity of vanadium samples could be attributed to the higher lability and consequently easier removal of lattice oxygen from  $\text{VO}_x$  moieties. The Tamman temperature of metal oxides can be used as a qualitative measurement of oxygen mobility.  $\text{V}_2\text{O}_5$  has a lower Tamman temperature than  $\text{MoO}_3$  (208 and 261 °C, respectively), indicating the higher lability of lattice oxygen in  $\text{VO}_x$  catalysts [34].

The relative ease in the removal of lattice oxygen, which presumably leads to high activity, is frequently characterized by the ease of catalyst reduction with hydrogen. On  $\text{MoO}_x$  and  $\text{VO}_x$  catalysts, propane ODH rates were found to increase as the reducibility of the metal cations increased [11]. On the other hand, there are studies reporting that the trend in TOF values does not follow the reducibility of the surface metal oxide species. Kim et al. [12] reported that in the case of methanol oxidation, the extent of surface reduction during reaction does not follow the trend observed during temperature programmed reduction with hydrogen. According to Banares [2], these disagreements arise from the fact that some reports correlate activity with the bulk reducibility of the catalyst, which may differ significantly from that of the surface sites and lead to different conclusions.

The results of the TPR studies performed in this work also do not allow a correlation between bulk reducibility–activity, since all catalysts exhibit similar reduction behavior, with the  $T_{\text{max}}$  of hydrogen consumption ranging between 490–520 °C, but dramatically different activity. This observation is in line with previous studies on  $\text{MoO}_3/\text{Al}_2\text{O}_3$  catalysts, where catalysts with different reduction behavior were found to have the same reactivity in ethane ODH [35]. Chen et al. have recently reported the significant variation in propane ODH rates over different metal oxides with similar  $\text{H}_2$  reduction rates. The authors suggest that the  $\text{H}_2$  reduction process is dissimilar to the redox cycles required for alkane ODH, thus no direct relationship between the two processes can be established [33]. It seems that temperature programmed reduction profiles reflect the structural transformation of the starting high valence oxides into structurally distinct suboxides, instead of merely the ease of removal of the few oxygen atoms generally missing during steady state ODH reaction. Anniballi et al., who also found no correlation between reducibility and activity during propane ODH, offer another explanation. The authors claim that what could have a major effect on the activity in

oxidative dehydrogenation reaction is the re-oxidation and not the reduction of the catalyst during reaction conditions [36].

An excellent correlation between the UV–visible absorption-edge energies of the catalysts and propane ODH rates was established by Chen et al. [33]. The authors suggest that the absorption-edge energy, which reflects the energy required for electronic transitions in metal oxides, can be used to characterize the ease of C–H activation by each metal oxide, since the activation of the alkane C–H bond involves the transfer of electrons from lattice oxygen to metal cations. Indeed, in Mo catalysts the energy required for these electron transfers was higher accounting for the lower reactivity, compared to V catalysts, which exhibited low absorption-edge energies.

### 4.2. Effect of support

As far as the nature of the support is concerned, titania-supported  $\text{MO}_x$  (M=Mo, V) catalysts exhibit generally higher reactivity than the corresponding alumina ones. The Raman spectra presented in this work show that the structure of the supported  $\text{MoO}_x$  domains at monolayer coverage on titania and alumina are very similar, with the co-existence of monomeric and polymeric  $\text{MoO}_x$  units. Our results are in agreement with results from Wachs and co-workers, who have extensively investigated the structure of molybdenum-oxo species dispersed on several supports by in situ Raman spectroscopy [12,17]. They found that at monolayer coverage on  $\text{Al}_2\text{O}_3$ , highly distorted polymerized surface molybdenum oxide species in octahedral coordination coexisted with tetrahedral, isolated surface species. On  $\text{TiO}_2$ , the  $\text{MoO}_x$  species were found to be less polymerized than on  $\text{Mo}/\text{Al}_2\text{O}_3$ . Nevertheless, the similarity of the Mo–O vibrations confirmed the presence of Mo species with no significant difference in structure.

In the case of vanadia deposition on alumina and titania, we observed a small differentiation in the species formed on the catalyst surface. Titania was found to be more effective for the formation of amorphous well-dispersed  $\text{VO}_x$  species, while on alumina  $\text{V}_2\text{O}_5$  and  $\text{AlVO}_4$  crystallites were formed. The high dispersion of vanadia on titania could be due to increased formation of  $\text{VO}_x$  oligomers, as opposed to larger polyvanadate domains which prevail on the surface of alumina acting as precursors for the formation of oxide crystallites [28,30,31]. However, concerning the amorphous  $\text{VO}_x$  structure, vanadium loading close to monolayer leads to the co-existence of similar monovanadate and polyvanadate structures on both supports.

Hence, it is clear that the variation in the activity of titania- and alumina-supported  $\text{MO}_x$  catalysts is not a structural factor and cannot be solely related to the configuration of the surface metal oxide species. Differences in the activity of vanadia species supported on different metal oxides have been attributed to the V–O–support bond, which has been claimed to be the kinetically relevant bond. The participation



of the terminal V=O bond as the critical site for propane oxidative dehydrogenation has been ruled out, by means of in situ Raman techniques, whereas V–O–V bonds were found not to be critical for this reaction [29,37]. The direct involvement of the V–O–support bond in the rate-determining step of ODH of propane is sustained. Routray et al. [38] have also attributed the catalytic activity and reducibility to the V–O–S bond. It seems that V–O–S determines the magnitude of the pre-exponential factor. Therefore, the rate that the catalytic reduction–oxidation cycles occur during alkane ODH is strongly dependent on the specific oxide support used to support the surface vanadium oxide species.

The presence of smaller domains on the titania support surface, as evidenced by Raman measurements, indicates the increased amount of Me–O–S bonds, related with the fine dispersion of the metals on the support surface, which could explain the increased reactivity of the 5VTi catalyst. In situ Raman studies performed by our group on V/TiO<sub>2</sub> and V/ZrO<sub>2</sub> catalysts in propane ODH support this conclusion [28].

Moreover, the higher reactivity of VTi can be ascribed to the easier removal of oxygen from the V–O–Ti bonds compared to the V–O–Al bonds present in the VAl catalyst. The same conclusion can be drawn out for molybdena catalysts. This in turn can be related to the electronegativity of the support cation (Al or Ti). According to Burcham et al. [26], there is a correlation between the TOF and the ligand cation electronegativity, with the more electropositive supports leading to higher catalytic activity, a statement which is in agreement with our results. A theoretical approach could be that the higher the difference between the electronegativity of active metal cation or support cation with oxygen, the stronger the bond. The oxygen in the V–O–support bond is more negatively charged in the case of the less electronegative Ti (1.54) compared to Al (1.61), thus more reactive towards the alkane C–H bonds. Although the support effect is significantly less for the Mo catalysts, the same explanation can be offered.

#### 4.3. Effect of nature of alkane

A quick comparison between the catalytic results obtained with ethane/oxygen and propane/oxygen mixtures shows that the ODH rates accomplished are in general 3–4 times higher when propane is used as feedstock than for ethane. Since the C–H bond in the alkane is the rate-determining step of the reaction, the reason for this predictable result is quite straightforward and can be easily explained by the simple chemistry of the two molecules. The ethane molecule consists of only primary C–H bonds, which have energy of 420 kJ/mol [10]. Propane has two weaker secondary bonds (401 kJ/mol), which render propane more reactive and easier to activate at lower temperatures than ethane. However, the ethane oxidative dehydrogenation reaction is as a rule more selective than propane ODH. Higher selectivities to C<sub>2</sub>H<sub>4</sub> compared to C<sub>3</sub>H<sub>6</sub> were observed in the whole range of reaction conditions for all the catalysts tested. The lower values of propene se-

lectivity compared to ethene can be explained by the weaker C–H bonds and the C–C bond cleavage in propane. The selectivity to propylene at zero propane conversion is lower than the initial ethylene selectivity, proving that during propane ODH, the primary reactions to carbon oxides are more extensive than in ethane ODH. The chemistry of the produced alkenes also accounts for the more efficient production of ethene than propene. Ethene is the only alkene that possesses only strong vinylic C–H bonds (445 kJ/mol) and as a result is relatively stable and not easily prone to further oxidation. The allylic bonds (361 kJ/mol) make propene much more reactive relative to propane than ethene is to ethane [10].

According to the previous, higher activation energies would be expected for ethane than for propane reactions. The Arrhenius plots for ethane and propane consumption rates over the four catalysts under study are compiled in Fig 9A and B, respectively. The calculated apparent activation energies are listed in Table 2. Surprisingly, the energy required for the activation of ethane and propane is very similar. Since, as already mentioned, the secondary C–H bonds in propane are weaker than the primary C–H bonds in ethane, other factors must account for the equivalence of the activation energies. One of these factors may be the stability of the intermediate species formed upon C–H bond activation. In situ IR studies performed over MoAl catalyst for the oxidative dehydrogenation of ethane indicated ethoxide species to be intermediates in the reaction mechanism [39]. Since the ODH of ethane and propane seem to proceed via the same mechanism, isopropoxides can be proposed as analogous intermediate species when propane is used as feed. Higher stabilization energy for ethoxide than isopropoxide species could compensate for the differences in C–H bond energies in the transition state involved in C–H bond activation and lead to similar activation energies for the two alkane reactants. These results coincide with results of Argyle et al., who reported same activation energies for ethane and propane dehydrogenation on alumina-supported vanadia catalysts [32].

We already discussed that the activation of the alkane C–H bond, the rate-determining step of the reaction, involves the transfer of two electrons from lattice oxygen to the metal cations. The electrons can be transferred to either one metal cation, leading to a two-electron reduction ( $M^{n+} \rightarrow M^{(n-2)+}$ ), or to two cations, which undergo a one-electron reduction ( $M^{n+} \rightarrow M^{(n-1)+}$ ). The latter case is the most energetically favored and the reaction will follow the pathway with the lowest energetic requirements. Alkanes with longer carbon chain can more easily coordinate to two adjacent M atoms. This could also be a possible explanation for the higher reactivity of propane in respect to ethane, which would need more dense M sites for effective activation. Moreover, it has been proposed that the distance between active sites influences the selectivity in the ODH of *n*-butane, while propane, with a shorter chain of C atoms, is less sensitive to this effect [14]. One can assume that ethane is even less sensitive than propane, due to an even lower carbon chain, and this could be

another reason for the higher selectivity recorded in ethane ODH. The distance of the active sites could control the oxidation of the adsorbed paraffin and/or the overoxidation of the primarily produced alkene.

## 5. Conclusions

Mo and V catalysts supported on titania and alumina at theoretical monolayer coverage were tested in the oxidative dehydrogenation of ethane and propane. Characterization of the materials showed that  $\text{MoO}_x$  and  $\text{VO}_x$  surface species are essentially amorphous in nature and well dispersed on the support surface in isolated and polymeric moieties, with the exception of the  $\text{VO}_x/\text{Al}_2\text{O}_3$  catalyst where formation of crystalline  $\text{V}_2\text{O}_5$  and mixed  $\text{AlVO}_4$  phase was also observed. Acidity measurements showed that the catalytic materials possess acid sites of weak and moderate strength.  $\text{MO}_x$  ( $\text{M} = \text{Mo}, \text{V}$ ) species supported on  $\text{TiO}_2$  exhibited in general higher acidity than the corresponding  $\text{Al}_2\text{O}_3$  supported ones, while V catalysts were more acidic than the corresponding Mo ones on the same support.

Vanadia catalysts were more active than molybdena catalysts in the oxidative dehydrogenation of both ethane and propane, irrespective of the support used. No correlation between bulk reducibility, determined by TPR, and activity was established, since all catalysts exhibited similar reduction behavior with  $T_{\text{max}}$  ranging between 490 and 520 °C, but dramatically different activity.

Comparing catalysts on different supports, catalysts supported on titania were more active and less selective than those supported on alumina, indicating the great impact of the support on the catalytic performance. Taking into account that the critical bond for the ODH reaction is the metal–O–support bond, the formation of polymeric entities with smaller chains (oligomers), especially on the vanadia on titania catalyst, indicates the increased amount of Me–O–S bonds and explains the higher reactivity to the reaction. Moreover, a correlation between reactivity and ligand cation electronegativity, with the more electropositive support leading to higher catalytic activity, was established.

In the whole range of the experiments performed, propane was much more reactive than ethane, exhibiting the same alkane conversion at temperatures lower by even 100 °C at the same residence time. Although the trend of the activation energies follows the catalytic results in both cases (ethane and propane ODH), the comparison between ethane and propane is not what someone would predict. The activation energies for propane ODH would be expected to be lower than the ones for ethane ODH, since the C–H bond, whose activation is the kinetically relevant step, is weaker in the propane molecule. However, the calculated apparent activation energies for ethane and propane show similar values. One of the factors that make the results divert could be the stability of the intermediate radical formed upon C–H bond activation in ethane and propane.

## Acknowledgements

General Secretariat for Research and Technology is gratefully acknowledged for the financial support (PENED2001). The authors would like to thank Philipp Hauck from Technical University of Munich for his help with Raman measurements.

## References

- [1] G. Centi, F. Cavani, F. Trifiro, *Selective Oxidation by Heterogeneous Catalysis*, Kluwer Academic Publishers/Plenum Press, New York, 2001.
- [2] M.A. Banares, *Catal. Today* 51 (1999) 319.
- [3] T. Blasco, J.M. Lopez-Nieto, *Appl. Catal. A* 157 (1997) 117.
- [4] E.A. Mamedov, V. Cortes Corberan, *Appl. Catal. A* 127 (1995) 1.
- [5] A.A. Lemonidou, L. Nalbandian, I.A. Vasalos, *Catal. Today* 46 (2000) 333.
- [6] B. Grzybowska-Swierkosz, *Topics Catal.* 21 (2002) 35.
- [7] G. Deo, I.E. Wachs, *J. Catal.* 146 (1994) 323.
- [8] I.E. Wachs, B.M. Weckhuysen, *Appl. Catal. A* 157 (1997) 67.
- [9] A. Corma, J.M. Lopez Nieto, N. Paredes, M. Perez, Y. Shen, H. Cao, S.L. Suib, *Stud. Surf. Sci. Catal.* 72 (1992) 213.
- [10] H.H. Kung, *Adv. Catal.* 40 (1994) 1.
- [11] K. Chen, S. Xie, A.T. Bell, E. Iglesia, *J. Catal.* 198 (2001) 232.
- [12] D.S. Kim, I.E. Wachs, K. Segawa, *J. Catal.* 146 (1994) 268.
- [13] A. Galli, J.M. Lopez Nieto, A. Dejoz, M.I. Vazquez, *Catal. Lett.* 34 (1995) 51.
- [14] P.M. Michalakos, M.C. Kung, I. Jahan, H.H. Kung, *J. Catal.* 140 (1993) 226.
- [15] M.C. Abello, M.F. Gomez, O. Ferretti, *Appl. Catal. A* 207 (2001) 421.
- [16] E. Hillerova, H. Morishige, K. Inamura, M. Zdrzil, *Appl. Catal. A* 156 (1997) 1.
- [17] H. Hu, I.E. Wachs, S.R. Bare, *J. Phys. Chem. B* 99 (1996) 10897.
- [18] A. Khodakov, B. Olthof, A.T. Bell, E. Iglesia, *J. Catal.* 181 (1999) 205.
- [19] M.A. Banares, I.E. Wachs, *J. Raman Spectrosc.* 33 (2002) 259.
- [20] G. Mestl, T.K.K. Srinivasan, *Catal. Rev. Sci. Eng.* 40 (1998) 451.
- [21] F. Hardcastle, I.E. Wachs, *J. Phys. Chem.* 95 (1991) 5031.
- [22] N. Steinfeldt, D. Müller, H. Berndt, *Appl. Catal. A* 272 (2004) 201.
- [23] F. Roozeboom, M.C. Mittelmeijer-Hageleger, J.A. Moulijn, J. Medema, V.H.J. de Beer, P.J. Gellings, *J. Phys. Chem.* 84 (1980) 2783.
- [24] F. Arena, F. Frusteri, A. Parmaliana, *Catal. Lett.* 60 (1999) 59.
- [25] M.C. Abello, M.F. Gomez, M. Casella, O.A. Ferretti, M.A. Banières, J.L.G. Fierro, *Appl. Catal. A* 251 (2003) 435.
- [26] L.J. Burcham, M. Badlani, I.E. Wachs, *J. Catal.* 203 (2001) 104.
- [27] R. Grabowski, B. Grzybowska, K. Samson, J. Sloczynski, J. Stoch, K. Wcislo, *Appl. Catal. A* 125 (1995) 129.
- [28] A. Christodoulakis, M. Machli, A.A. Lemonidou, S. Boghosian, *J. Catal.* 222 (2004) 293.
- [29] P. Courtine, E. Bordes, *Appl. Catal. A* 157 (1997) 45.
- [30] G.T. Went, S.T. Oyama, A.T. Bell, *J. Phys. Chem.* 94 (1990) 4240.
- [31] B. Olthof, A. Khodakov, A.T. Bell, E. Iglesia, *J. Phys. Chem. B* 104 (2000) 1516.
- [32] M.D. Argyle, K. Chen, A.T. Bell, E. Iglesia, *J. Catal.* 208 (2002) 139.
- [33] K. Chen, A. Bell, E. Iglesia, *J. Catal.* 209 (2002) 35.
- [34] K. Chen, A.T. Bell, E. Iglesia, *J. Phys. Chem. B* 104 (2000) 1292.
- [35] E. Heracleous, J. Vakros, A.A. Lemonidou, Ch. Kordulis, *Catal. Today* 91–92C (2004) 289.

- [36] S. Anniballi, F. Cavani, A. Guerrini, B. Panzacchi, F. Trifirò, C. Fumagalli, R. Leanza, G. Mazzoni, *Catal. Today* 78 (2003) 117.
- [37] G. Mul, M.A. Banares, G. Garcia Cortez, B. van der Linden, S.J. Khatib, J.A. Moulijn, *PCCP* 20 (2003) 4378.
- [38] K. Routray, K.R.S.K. Reddy, G. Deo, *Appl. Catal. A* 265 (2004) 103.
- [39] E. Heracleous, A.A. Lemonidou, J.A. Lercher, *Appl. Catal. A* 264 (2004) 73.